



Copyright Notice

©2010 IEEE. Personal use of this material is permitted. However, permission to reprint/republish this material for advertising or promotional purposes or for creating new collective works for resale or redistribution to servers or lists, or to reuse any copyrighted component of this work in other works must be obtained from the IEEE.

This document was downloaded from Chalmers Publication Library (<http://publications.lib.chalmers.se/>), where it is available in accordance with the IEEE PSPB Operations Manual, amended 19 Nov. 2010, Sec. 8.1.9 (<http://www.ieee.org/documents/opsmanual.pdf>)

(Article begins on next page)

Soft Demodulation Algorithms for Orthogonally Modulated and Convolutionally Coded DS-CDMA Systems

Pei Xiao, *Member, IEEE*, and Erik Ström, *Senior Member, IEEE*

Abstract—A convolutionally coded M -ary orthogonal direct sequence code division multiple access (DS-CDMA) system in time-varying frequency-selective Rayleigh fading channels is considered in this work. We propose several novel soft demodulation algorithms based on interference cancellation and suppression techniques that can be coupled with soft decoding to improve the system performance in an iterative manner. The performance of the proposed demodulation algorithms is evaluated numerically and proved to achieve substantial bit error rate (BER) performance gain compared with the conventional detection schemes.

I. INTRODUCTION

We study the orthogonally modulated DS-CDMA system with convolutional encoding. The orthogonal modulation is accomplished by Walsh code which combines the advantages of spreading and coding to achieve improved performance for spread spectrum (CDMA) systems. It was shown in [1, 2] that M -ary signaling significantly improves bandwidth efficiency compared with binary signaling in fading and nonfading channels, and the efficiency further improves as the order of multipath diversity increases. Joint M -ary orthogonal signal demodulation and channel decoding for similar systems was introduced in [3, 4]. However, only a single user scenario was considered in those papers, and some important issues, e.g., channel estimation and multiple access interference (MAI) mitigation were not addressed. In a conventional receiver, the interface between subsystems involves the passing of bits, or hard-decisions, down the stages of the chain. Whenever hard-decisions are made, reliability information is lost and becomes unavailable to subsequent stages [7]. It is a well-known fact that soft-decision decoding outperforms hard-decision decoding by approximately 2 dB in AWGN channel, and the coding gain is even greater in presence of fading [8]. With emphasis on the development of soft demodulation algorithms to enable soft-decision decoding, we provide a more thorough treatment of joint multiuser detection, channel estimation, demodulation and decoding for this orthogonally modulated and convolutionally coded DS-CDMA system.

II. SYSTEM MODEL

The block diagram of the transmitter is shown in the upper part of Figure 1. The k^{th} user's l^{th} information

Dr. Pei Xiao is with the Institute of Electronics, Communications and Information Technology (ECIT), Queen's University Belfast, BT3 9DT, UK and Prof. Erik Ström is with the department of Signals and Systems, Chalmers University of Technology, SE-412 96 Gothenburg, Sweden. E-mails: pei.xiao@qub.ac.uk, erik.strom@chalmers.se

bit is denoted as $b_l^k \in \{+1, -1\}$ ($k = 1, \dots, K$, $l = 1, \dots, L_b$, where L_b is the block length). The information bits are encoded by a rate $R_c = 1/n_c$ convolutional encoder into the code bits $u_{n,l}^k \in \{+1, -1\}$, where $u_{n,l}^k$, $n = 0, 1, \dots, n_c$ denotes the code bits of the trellis transition that is due to b_l^k . Code bits are subsequently interleaved and each block of $\log_2 M$ coded and interleaved bits $u_{n,l}^k \in \{+1, -1\}$ is mapped into $\mathbf{w}_{i_k(j)} \in \{\mathbf{w}_0, \dots, \mathbf{w}_{M-1}\}$, which is one of the M Walsh code-words. The subscript $i_k(j) \in \{0, 1, \dots, M-1\}$ denotes the k^{th} user's j^{th} Walsh symbol index. The Walsh code-word $\mathbf{w}_{i_k(j)} \in \{+1, -1\}^M$ is then repetition encoded into $\mathbf{s}_k(j) = \text{rep}(\mathbf{w}_{i_k(j)}, N/M) \in \{+1, -1\}^N$, where $\text{rep}(\cdot, \cdot)$ denotes the repetition encoding operation, whose first argument is the input bits and the second one is the repetition factor. The Walsh sequence $\mathbf{s}_k(j)$ is then scrambled by a scrambling code unique to each user to form the transmitted chip sequence $\mathbf{a}_k(j) = \mathbf{C}_k(j)\mathbf{s}_k(j) \in \{+1, -1\}^N$, where $\mathbf{C}_k(j) \in \{-1, +1\}^{N \times N}$ is a diagonal matrix whose diagonal elements correspond to the scrambling code for the k^{th} user's j^{th} symbol. The purpose of scrambling is to separate users. The scrambled sequence $\mathbf{a}_k(j)$ is pulse amplitude modulated to form the baseband signal, which is multiplied with a carrier and transmitted over a Rayleigh fading channel with L_k resolvable paths, having time-varying complex channel gains $h_{k,1}(t), h_{k,2}(t), \dots, h_{k,L_k}(t)$, and delays $\tau_{k,1}, \tau_{k,2}, \dots, \tau_{k,L_k}$ ¹. We assume that the channel time variation is slow compared to the symbol duration T , i.e., $h_{k,l}(t) \approx h_{k,l}(jT)$ for $jT \leq t < (j+1)T$. After frequency down-conversion and chip matched filtering, the received signal corresponding to the k^{th} user's j^{th} transmitted Walsh sequence $\mathbf{s}_k(j)$ can be written in vector form as

$$\begin{aligned} \mathbf{r}_k(j) &= \mathbf{A}_k(j)\mathbf{h}(j) + \mathbf{n}(k, j) \\ &= \mathbf{X}_k(j)\mathbf{h}_k(j) + \text{ISI}_k(j) + \text{MAI}_k(j) + \mathbf{n}_k(j) \in \mathbb{C}^{N_k}, \end{aligned} \quad (1)$$

where $N_k = N + p_{k,L_k} - p_{k,1}$, and the columns of the matrix $\mathbf{A}_k(j) \in \mathbb{R}^{N_k \times L_{\text{tot}}}$ ($L_{\text{tot}} = \sum_{k=1}^K L_k$) are the delayed versions of the transmitted chip sequences $\mathbf{a}_k(j)$ for $k = 1, 2, \dots, K$, one column per path. The symbols \mathbb{C} and \mathbb{R} denote the complex and real fields, respectively. The length of the processing window N_k is larger than the symbol interval N to account for the asynchronous and multipath nature of the channel. The columns are

¹Assume $\tau_{k,l} = (p_{k,l} + \delta_{k,l})T_c$, where T_c is the chip duration, $p_{k,l} \in \mathbb{Z}$ and $\delta_{k,l} \in [0, 1)$ are the integer and fractional parts of the delay $\tau_{k,l}$, respectively.

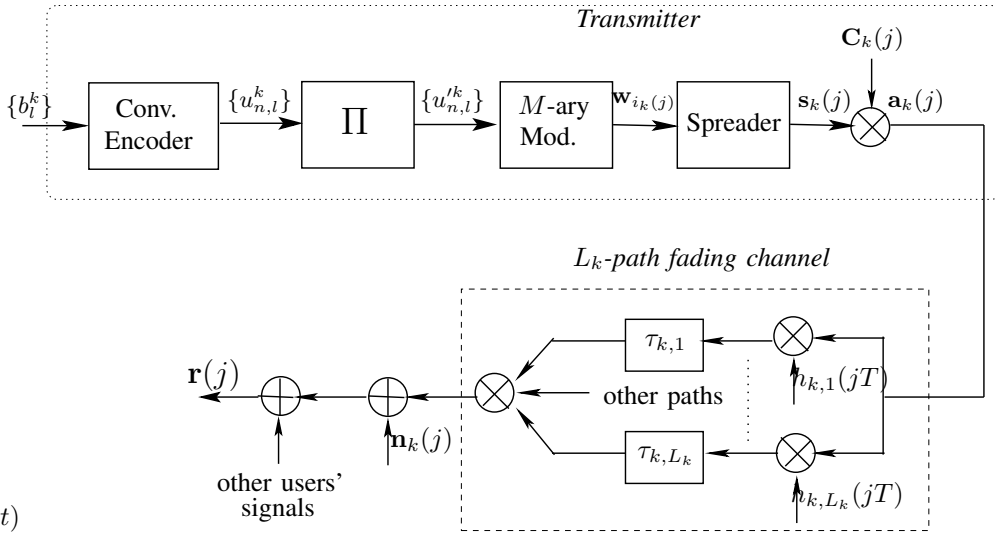


Fig. 1. The baseband equivalent block diagram for the transmitter and the multipath channel.

weighted by the channel vector $\mathbf{h}(j) \in \mathbb{C}^{L_{\text{tot}}}$, which is defined as

$$\begin{aligned} \mathbf{h}(j) &= [\mathbf{h}_1^T(j) \quad \mathbf{h}_2^T(j) \quad \cdots \quad \mathbf{h}_{K'}^T(j)]^T, \\ \mathbf{h}_i(j) &= [h_{k,1}(jT) \quad h_{k,2}(jT) \quad \cdots \quad h_{k,L_k}(jT)]^T. \end{aligned} \quad (2)$$

The received vector $\mathbf{r}_k(j)$ can be written as the sum of four terms: the signal of interest $\mathbf{X}_k(j)\mathbf{h}_k(j)$, the intersymbol interference (ISI), the multiple access interference (MAI), and the thermal noise. The columns of the matrix $\mathbf{X}_k(j) \in \mathbb{R}^{N_k \times L_k}$ are essentially the shifted versions of the chips due to the k^{th} user's j^{th} symbol, one column per path. The noise term $\mathbf{n}_k(j)$ is a vector of complex noise samples with zero mean and variance N_0 . We refer to [5] for a quantified information about the ISI and MAI as well as a detailed description of the system model.

The task of the receiver is to detect the information bits transmitted from all users, i.e., detect b_l^k given the observation $\mathbf{r}(k, j)$, for $k = 1, 2, \dots, K$ and $j = 1, 2, \dots, \frac{L_b}{R_c \log_2 M}$, where R_c is the code rate of the employed convolutional code. The proposed iterative soft demodulation and decoding scheme is illustrated in Figure 2. The demodulator and decoder are each implemented with a soft-input, soft-output (SISO) algorithm and operate in an iterative feedback mode. The soft metric $\lambda(u_{n,l}^k; O)$ from the demodulator is deinterleaved to $\lambda(u_{n,l}^k; I)$. The k^{th} user's Log-MAP decoder [6] computes a posteriori LLR of each information bit $\lambda(b_l^k; O)$ and each code bit $\lambda(u_{n,l}^k; O)$ based on the soft input $\lambda(u_{n,l}^k; I)$ and the trellis structure of the convolutional code. The former is used to make a decision on b_l^k at the final iteration, while $\lambda(u_{n,l}^k; O)$ is used for channel estimation and interference cancellation/suppression in the demodulator at the next iteration. The notations $\lambda(\cdot; I)$ and $\lambda(\cdot; O)$ are used to denote the input and output ports of a SISO device.

III. SOFT DEMODULATION ALGORITHMS

In this section, we discuss the design of soft demodulators that can produce soft reliability values for each bit $u_{n,l}^k$ from the received vector $\mathbf{r}_k(j)$ in order to enable soft input channel decoding. The soft metric for the bit $u_{n,l}^k$ is computed as

$$\begin{aligned} \lambda(u_{n,l}^k; O) &= \ln \frac{\sum_{m: u_{n,l}^k = +1} f(\mathbf{r} | \mathbf{w}_m)}{\sum_{m: u_{n,l}^k = -1} f(\mathbf{r} | \mathbf{w}_m)} \\ &= \ln \frac{\sum_{m: u_{n,l}^k = +1} f(\mathbf{r} | \mathbf{s}_m)}{\sum_{m: u_{n,l}^k = -1} f(\mathbf{r} | \mathbf{s}_m)} \\ &\approx \ln \frac{\max_{m: u_{n,l}^k = +1} f(\mathbf{r} | \mathbf{s}_m)}{\max_{m: u_{n,l}^k = -1} f(\mathbf{r} | \mathbf{s}_m)}, \end{aligned} \quad (3)$$

where $m : u_{n,l}^k = \pm 1$ denotes the set of Walsh sequences $\{\mathbf{s}_m\}$ that correspond to the code bit $u_{n,l}^k = \pm 1$. The approximation in (3) is due to the fact that typically one term will dominate each sum in (3), which suggests the “dual-maxima” rule. The derivation of different soft demodulation schemes will be given below. To simplify the notation, we suppress the index k and/or j from $\mathbf{s}_k(j)$, $\mathbf{C}_k(j)$, $\mathbf{r}_k(j)$, $\mathbf{A}_k(j)$, $\mathbf{n}_k(j)$, $\mathbf{X}_k(j)$ and $\mathbf{h}_k(j)$, etc., whenever no ambiguity arises.

A. Soft Demodulation with Matched Filter (MF)

Let $\mathbf{r}_{k,l}$ ($l = 1, 2, \dots, L_k$) denote the delay aligned version of the received vector due to the transmission of the j^{th} symbol from the k^{th} user's l^{th} path and denote the vector $\tilde{\mathbf{r}}_{k,l} \in \mathbb{C}^N$ as $\mathbf{r}_{k,l}$ descrambled with the scrambling sequence \mathbf{C}_k . The descrambled vector $\tilde{\mathbf{r}}_{k,l}$ can be expressed as $\tilde{\mathbf{r}}_{k,l} = \mathbf{s}_k h_{k,l} + \mathbf{m}_{k,l} + \mathbf{i}_{k,l} + \mathbf{n}_{k,l}$, where $\mathbf{s}_k \in \{\mathbf{s}_0, \mathbf{s}_1, \dots, \mathbf{s}_{M-1}\}$ is the transmitted Walsh sequence. The desired signal vector $\mathbf{s}_k h_{k,l}$ is due to the contribution from the k^{th} user's l^{th} path. The vectors $\mathbf{m}_{k,l}$ and $\mathbf{i}_{k,l}$ represent the MAI and ISI terms, respectively. It was shown in [5] that both the MAI and ISI terms can be

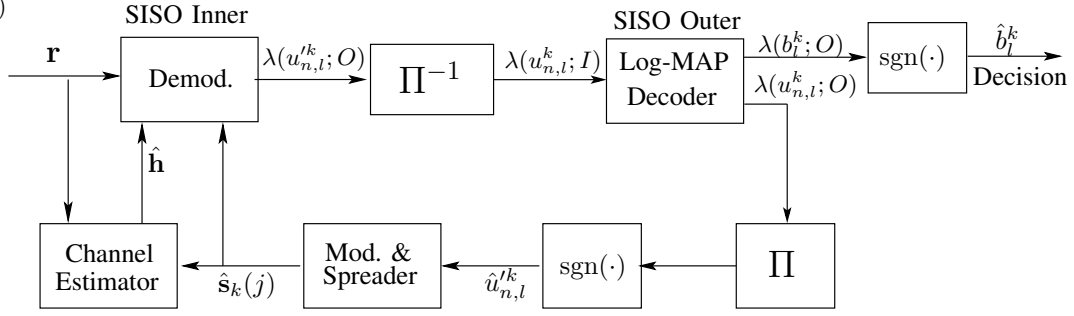


Fig. 2. Iterative soft demodulation and Log-MAP decoding. The interleaver and deinterleaver are denoted as Π and Π^{-1} , respectively.

approximated as independent complex Gaussian random vectors: $\mathbf{m}_{k,l} \in \mathcal{CN}(\mathbf{0}, \sigma_m^2 \mathbf{I}_N)$ and $\mathbf{i}_{k,l} \in \mathcal{CN}(\mathbf{0}, \sigma_i^2 \mathbf{I}_N)$. Therefore, $\tilde{\mathbf{r}}_{k,l}$ can be reformulated as $\tilde{\mathbf{r}}_{k,l} = \mathbf{s}_k h_{k,l} + \tilde{\mathbf{n}}_{k,l}$ where $\tilde{\mathbf{n}}_{k,l} = \mathbf{m}_{k,l} + \mathbf{i}_{k,l} + \mathbf{n}_{k,l} \in \mathbb{C}^N$ follows $\tilde{\mathbf{n}}_{k,l} \sim \mathcal{CN}(\mathbf{0}, N'_0 \mathbf{I}_N)$ and $N'_0 = \sigma_m^2 + \sigma_i^2 + \sigma_n^2$. According to [5], $\sigma_n^2 = NN_0$, and

$$\sigma_i^2 = \sum_{q=1}^{L_k} \sum_{n=1}^N \mathbb{E}[|h_{k,q}|^2] = N \sum_{\substack{q=1 \\ q \neq l}}^{L_k} P_{k,q};$$

$$\sigma_m^2 = \sum_{p=1}^K \sum_{q=1}^{L_p} \sum_{n=1}^N \mathbb{E}[|h_{p,q}|^2] = N \sum_{\substack{p=1 \\ p \neq k}}^K \sum_{q=1}^{L_p} P_{p,q},$$

for chip synchronous systems, where $P_{k,i}$ is the power of $h_{k,i}$. Note that σ_i depends on k and l and that σ_m depends on k . The variances of MAI and ISI for chip asynchronous systems differ by a factor of $2/3$ [5]. Also, the noise terms $\tilde{\mathbf{n}}_{k,1}, \dots, \tilde{\mathbf{n}}_{k,L_k}$ are approximately uncorrelated after despreading due to descrambling. Thus,

$$f(\mathbf{r}|\mathbf{s}_m) = \prod_{l=1}^{L_k} f(\tilde{\mathbf{r}}_{k,l}|\mathbf{s}_m); \quad \text{where}$$

$$f(\tilde{\mathbf{r}}_{k,l}|\mathbf{s}_m) = \frac{1}{(\pi N'_0)^N} \exp\left(-\frac{\|\tilde{\mathbf{r}}_{k,l} - \mathbf{s}_m h_{k,l}\|^2}{N'_0}\right);$$

$$\lambda_{\text{MF}}^C(u_{n,l}^k; O) \approx \ln \frac{\max_{m:u_{n,l}^k=+1} \prod_{l=1}^{L_k} f(\tilde{\mathbf{r}}_{k,l}|\mathbf{s}_m)}{\max_{m:u_{n,l}^k=-1} \prod_{l=1}^{L_k} f(\tilde{\mathbf{r}}_{k,l}|\mathbf{s}_m)}$$

$$= \frac{2}{N'_0} \sum_{l=1}^{L_k} \text{Re} \{h_{k,l}^* \mathbf{s}^{+,*} \tilde{\mathbf{r}}_{k,l} - h_{k,l}^* \mathbf{s}^{-,*} \tilde{\mathbf{r}}_{k,l}\}. \quad (4)$$

In Equation (4), \mathbf{s}^+ denotes the Walsh sequence \mathbf{s}_m that corresponds to $\max_{m:u_{n,l}^k=+1} f(\mathbf{r}|\mathbf{s}_m)$, and \mathbf{s}^- is defined similarly. The superscript operator $(\bullet)^*$ is the conjugate transpose operation when applied to matrices, and simply the conjugate when applied to scalars.

A non-coherent version of the MF soft demodulator can be obtained similarly in a path-by-path manner as

$$\lambda_{\text{MF}}^N(u_{n,l}^k; O) \approx \sum_{l=1}^{L_k} |\mathbf{s}^{+,*} \tilde{\mathbf{r}}_{k,l}| - \sum_{l=1}^{L_k} |\mathbf{s}^{-,*} \tilde{\mathbf{r}}_{k,l}|. \quad (5)$$

An estimate of the complex channel gain $h_{k,l}$ is not needed to compute the LLR value for bit $u_{n,l}^k$ in (5). This is particularly useful at the beginning of the iteration process when the estimate of channel fading is not yet available. The coherent MF demodulator expressed by (4) is applicable only when pilot symbols are available for channel estimation.

B. Soft Demodulation with Interference Cancellation (IC)

Once the transmitted signals are estimated for all the users at the previous iteration, the interference can be removed by subtracting the estimated signals of the interfering users from the received signal \mathbf{r} to form a new signal vector \mathbf{r}' for demodulating the signal transmitted from user k , i.e., $\mathbf{r}' = \mathbf{r} - \hat{\mathbf{y}} + \hat{\mathbf{X}}_k \hat{\mathbf{h}}_k$, where $\mathbf{r} \in \mathbb{C}^{N_k}$ denotes the received signal vector due to the transmission of the j^{th} symbol from the k^{th} user, and $\mathbf{r}' \in \mathbb{C}^{N_k}$ is its interference cancelled version after subtracting the contributions from all the other users using decision feedback. The vector $\hat{\mathbf{y}} = \hat{\mathbf{A}} \hat{\mathbf{h}}$ represents the estimated contribution from all the users calculated by using the data matrix $\hat{\mathbf{A}}$ and channel vector $\hat{\mathbf{h}}$ estimated at the previous iteration. The vector $\hat{\mathbf{X}}_k \hat{\mathbf{h}}_k$ is the estimated contribution from all the paths of user k . In case of perfect cancellation, \mathbf{r}' only contains the contribution from the k^{th} user plus original additive Gaussian noise $\mathbf{n} \in \mathbb{C}^{N_k}$, i.e., $\mathbf{r}' = \mathbf{X}_k \mathbf{h}_k + \mathbf{n}$. Its conditional probability density function (PDF) can be expressed as $f(\mathbf{r}'|\mathbf{s}_m) = \frac{1}{(\pi N_0)^{N_k}} \exp\left(-\frac{\|\mathbf{r}' - \mathbf{X}_{k,m} \mathbf{h}_k\|^2}{N_0}\right)$. Therefore,

$$\lambda_{\text{IC}}(u_{n,l}^k; O) \approx \ln \frac{\max_{m:u_{n,l}^k=+1} f(\mathbf{r}'|\mathbf{s}_m)}{\max_{m:u_{n,l}^k=-1} f(\mathbf{r}'|\mathbf{s}_m)}$$

$$= \ln \frac{\exp(-\|\mathbf{r}' - \mathbf{X}^+ \mathbf{h}_k\|^2/N_0)}{\exp(-\|\mathbf{r}' - \mathbf{X}^- \mathbf{h}_k\|^2/N_0)}$$

$$= \frac{2}{N_0} \text{Re} \{ \mathbf{h}_k^* \mathbf{X}^{+,*} \mathbf{r}' - \mathbf{h}_k^* \mathbf{X}^{-,*} \mathbf{r}' \}, \quad (6)$$

where $\mathbf{X}_{k,m} = [\mathbf{x}_{k,1,m} \quad \mathbf{x}_{k,2,m} \quad \dots \quad \mathbf{x}_{k,L_k,m}]$, and $\mathbf{x}_{k,l,m}$ denotes the transmitted chip sequence due to the k^{th} user's j^{th} symbol from the l^{th} path based on the hypothesis that the m^{th} Walsh symbol is transmitted. In (6), \mathbf{X}^+ denotes the $\mathbf{X}_{k,m}$ that corresponds to $\max_{m:u_{n,l}^k=+1} f(\mathbf{r}'|\mathbf{s}_m)$, and \mathbf{X}^- denotes the $\mathbf{X}_{k,m}$ that corresponds to $\max_{m:u_{n,l}^k=-1} f(\mathbf{r}'|\mathbf{s}_m)$

C. Soft Demodulation with Interference Suppression (IS)

The idea of interference suppression (IS) is to suppress the estimated interference by filtering (orthogonal projection). We need to know (or estimate) the structure of the interference in order to construct the suppression filter. To this end, we define the matrix

$$\mathbf{U} = [\tilde{\mathbf{A}}_1 \quad \dots \quad \tilde{\mathbf{A}}_{k-1} \quad \tilde{\mathbf{A}}_{k+1} \quad \dots \quad \tilde{\mathbf{A}}_K] \in \mathbb{R}^{N_k \times (L_{\text{tot}} - L_k)},$$

where $\tilde{\mathbf{A}}_n$ is made up by the columns of \mathbf{A} in (1) that is due to the n^{th} user. We can suppress the interference by projecting \mathbf{r} on the null space of \mathbf{U} , i.e., by multiplying \mathbf{r} from the left with $\mathbf{P}_{\mathbf{U}}^\perp = \mathbf{I} - \mathbf{U}\mathbf{U}^\dagger$, where \mathbf{U}^\dagger denotes the left pseudoinverse² of \mathbf{U} . We note that $\mathbf{P}_{\mathbf{U}}^\perp \tilde{\mathbf{A}}_i = \mathbf{0}$ [10] for all $i \neq k$, and $\mathbf{P}_{\mathbf{U}}^\perp \mathbf{r} = \mathbf{P}_{\mathbf{U}}^\perp [\mathbf{A}\mathbf{h} + \mathbf{n}] = \sum_{i=1}^K \mathbf{P}_{\mathbf{U}}^\perp \tilde{\mathbf{A}}_i \mathbf{h}_i + \mathbf{P}_{\mathbf{U}}^\perp \mathbf{n} = \mathbf{P}_{\mathbf{U}}^\perp \tilde{\mathbf{A}}_k \mathbf{h}_k + \mathbf{P}_{\mathbf{U}}^\perp \mathbf{n}$. The interference is suppressed since the columns of $\mathbf{P}_{\mathbf{U}}^\perp$ are orthogonal to the subspace spanned by the MAI (columns of \mathbf{U}). We note that IS is only meaningful if $\mathbf{P}_{\mathbf{U}}^\perp \tilde{\mathbf{A}}_k \neq \mathbf{0}$, which we will assume to be true from now on. It can be easily shown that $\mathbf{P}_{\mathbf{U}}^\perp = \mathbf{P}_{\mathbf{U}}^{\perp*}$, and $\mathbf{P}_{\mathbf{U}}^\perp = \mathbf{P}_{\mathbf{U}}^{\perp*} \mathbf{P}_{\mathbf{U}}^\perp$. Since a linear transformation of a Gaussian random variable is still a Gaussian random variable, and the original noise vector has the statistics $\mathbf{n} \sim \mathcal{CN}(\mathbf{0}, N_0 \mathbf{I})$, the covariance matrix for the projected noise vector $\tilde{\mathbf{n}} = \mathbf{P}_{\mathbf{U}}^\perp \mathbf{n}$ is thus $E[\tilde{\mathbf{n}}\tilde{\mathbf{n}}^*] = E[\mathbf{P}_{\mathbf{U}}^\perp \mathbf{n} \mathbf{n}^* \mathbf{P}_{\mathbf{U}}^{\perp*}] = \mathbf{P}_{\mathbf{U}}^\perp (N_0 \mathbf{I}) \mathbf{P}_{\mathbf{U}}^{\perp*} = N_0 \mathbf{P}_{\mathbf{U}}^\perp$. The conditional PDF can be approximated as

$$\begin{aligned} f(\mathbf{P}_{\mathbf{U}}^\perp \mathbf{r} | \mathbf{s}_m) &\approx \gamma \exp[-(\mathbf{P}_{\mathbf{U}}^\perp \mathbf{r} - \mathbf{P}_{\mathbf{U}}^\perp \mathbf{X}_{k,m} \mathbf{h}_k)^* \\ &\quad (N_0 \mathbf{P}_{\mathbf{U}}^\perp)^{-1} (\mathbf{P}_{\mathbf{U}}^\perp \mathbf{r} - \mathbf{P}_{\mathbf{U}}^\perp \mathbf{X}_{k,m} \mathbf{h}_k)] \\ &= \gamma \exp \left[-\frac{(\mathbf{r} - \mathbf{X}_{k,m} \mathbf{h}_k)^* \mathbf{P}_{\mathbf{U}}^\perp (\mathbf{r} - \mathbf{X}_{k,m} \mathbf{h}_k)}{N_0} \right] \\ &= \gamma \exp \left[-\frac{\|\mathbf{P}_{\mathbf{U}}^\perp \mathbf{r} - \mathbf{P}_{\mathbf{U}}^\perp \mathbf{X}_{k,m} \mathbf{h}_k\|^2}{N_0} \right], \end{aligned}$$

where $\gamma = \frac{1}{(\pi)^{N_k} \det(N_0 \mathbf{P}_{\mathbf{U}}^\perp)}$. The LLRs can thus be computed as

$$\begin{aligned} \lambda_{\text{IS}}(u_{n,l}^k; O) &\approx \ln \frac{\max_{m: u_{n,l}^k = +1} f(\mathbf{r} | \mathbf{s}_m)}{\max_{m: u_{n,l}^k = -1} f(\mathbf{r} | \mathbf{s}_m)} \\ &\approx \ln \frac{\max_{m: u_{n,l}^k = +1} \exp(-\|\mathbf{P}_{\mathbf{U}}^\perp \mathbf{r} - \mathbf{P}_{\mathbf{U}}^\perp \mathbf{X}_{k,m} \mathbf{h}_k\|^2 / N_0)}{\max_{m: u_{n,l}^k = -1} \exp(-\|\mathbf{P}_{\mathbf{U}}^\perp \mathbf{r} - \mathbf{P}_{\mathbf{U}}^\perp \mathbf{X}_{k,m} \mathbf{h}_k\|^2 / N_0)} \\ &= \ln \frac{\exp(-\|\mathbf{P}_{\mathbf{U}}^\perp \mathbf{r} - \mathbf{P}_{\mathbf{U}}^\perp \mathbf{X}^+ \mathbf{h}_k\|^2 / N_0)}{\exp(-\|\mathbf{P}_{\mathbf{U}}^\perp \mathbf{r} - \mathbf{P}_{\mathbf{U}}^\perp \mathbf{X}^- \mathbf{h}_k\|^2 / N_0)} \\ &= \frac{2}{N_0} \text{Re} \{ \mathbf{h}_k^* \mathbf{X}^{+*} \mathbf{P}_{\mathbf{U}}^\perp \mathbf{r} - \mathbf{h}_k^* \mathbf{X}^{-*} \mathbf{P}_{\mathbf{U}}^\perp \mathbf{r} \}, \quad (7) \end{aligned}$$

where \mathbf{X}^+ denotes the $\mathbf{X}_{k,m}$ that corresponds to $\max_{m: u_{n,l}^k = +1} f(\mathbf{P}_{\mathbf{U}}^\perp \mathbf{r} | \mathbf{s}_m)$, and \mathbf{X}^- is defined similarly.

The complexity of distinct algorithms is compared in Table I, which shows the required number of complex multiplications/divisions, and additions/subtractions for one user's one symbol estimate corresponding to the calculation of LLRs for $\log_2 M$ coded bits. One can see from the table that the complexity of both MF and IC schemes is linear in the spreading factor N , the number

²Hence, \mathbf{U}^\dagger is, in general, computed from the singular value decomposition of \mathbf{U} [9], or in the special case when \mathbf{U} has full column rank as $\mathbf{U}^\dagger = (\mathbf{U}^* \mathbf{U})^{-1} \mathbf{U}^*$.

of multipath component L , and the number of users K . However, the IS scheme requires cubic complexity, mainly due to the matrix inverse operation in (7), which needs to be done at symbol rate.

IV. NUMERICAL RESULTS

In Figure 3, we compare the performance of the discussed algorithms with the IC and IS demodulators, respectively. In the simulations, we employ a rate $R_c = 1/3$ convolutional code with generator polynomials $(25, 33, 37)_8$, and free distance $d_f = 12$. For each block, 4620 coded bits are passed through a block interleaver of size 66×70 . Each group of 3 interleaved bits from each user is converted into one of $M = 8$ Walsh codewords spread to a total length of $N = 64$ chips. The channels are independent multipath Rayleigh fading channels with $L_k = 3$ and Clarke's power spectrum with normalized Doppler frequency $f_D T = 0.01$ for all users. The non-coherent MF soft demodulation is used at the first iteration of the iterative process to obtain an initial estimate of data for channel and interference estimation. Channel estimation is done after each iteration with the maximum likelihood (ML) approach presented in [11]. The integrated approach results are plotted after 6 iterations (excluding the initial non-coherent detection stage) since convergence is normally reached by then. The single user bound is obtained by the integrated demodulation and Log-MAP decoding in a single user environment. No multiuser interference is present, but iterative process is performed to improve the channel estimates. The simulation results are averaged over random fading, noise, delays, and scrambling codes with minimum of 50 blocks of data transmitted and at least 100 bit errors generated. With the tandem approach, the demodulation and decoding are carried out only once, there is no feedback from the decoder to the demodulator. The performance of the coherent MF (conventional MRC-RAKE receiver) expressed by (4) is also shown in Figure 3a. It is a genie-aided tandem approach assuming perfect channel state information (CSI). One can see that at high SNRs, the IC scheme effectively mitigates the effect of MAI and outperforms the MRC-RAKE solution by a large margin. Clearly, interference mitigation is needed to improve the demodulation performance. Replacing the tandem approach with an integrated approach also gives substantial improvement (over 1 dB as shown in Figures 3a and 3b).

In Figure 3a, we also show the performance of the IC demodulator with and without the dual-maxima approximation in Equation (3). One can see that the performance loss due to the approximation is negligible compared to the exact implementation. The dual-maxima approximation is therefore used in the rest of simulations to simplify the computation of the LLR values for the demodulation schemes.

The IC and the IS demodulators are compared in Figure 3c under the same system setting as mentioned above. Apparently, the IC demodulator produces better

TABLE I

COMPLEXITY FOR ONE USER'S ONE SYMBOL ESTIMATE AT ONE ITERATION FOR THE ITERATIVE MUD ALGORITHMS CONSIDERED.

operations	\times/\div	$+/-$
MF	$NML + N$	$(N - 1)ML + \log_2 M$
IC	$N(ML + 2M + 2)$	$NML + NK - M + \log_2 M$
IS	$2(K - 1)^3 L^3 + (2N + 2)(K - 1)^2 L^2 + N^2(K - 1)L + N^2 M + N(ML + 2M + 2)$	$2(K - 1)^3 L^3 + (2N - 1)(K - 1)^2 L^2 + (N^2 - N)(K - 1)L + NM(L + N - 1) - M + \log_2 M$

results than the IS demodulator. For example, to achieve a target BER = 10^{-4} , $E_b/N_0 \approx 6.5$ dB is required with the integrated IC-LogMAP approach; while $E_b/N_0 \approx 9$ dB is required with the integrated IS-LogMAP approach. The same conclusion applies to the tandem approach as well. In both cases, the performance improvement provided by the IC scheme is over 2 dB. Also shown in Figure 3c is the error floor due to the non-coherent MF demodulator. Despite its poor performance, the non-coherent MF produces an initial estimate of data at the beginning of the iterative process to facilitate channel estimation and coherent demodulation in the subsequent stages. It can be seen from Figure 3 that the performance of the IC scheme is very close to the single user bound, which is not the case for the IS scheme. The relative poor performance of IS is due to the SNR loss by the projection of the received vector whenever the desired signal is not orthogonal to the interference (which is the case in all investigated scenarios).

In Figure 4, we compare the performance between the CDMA system with M -ary orthogonal signaling and the conventional CDMA system with binary signaling. Only the IC demodulation scheme is considered here since it has better performance and lower complexity than the IS scheme as analyzed earlier. The derivation for the detection schemes expressed by (4) and (6) are still valid for the conventional CDMA system, with the final expression for the coherent MF reformed as

$$\lambda_{\text{MF}}(u_{n,l}^k; O) \approx \frac{4}{N_0} \sum_{l=1}^{L_k} \text{Re} \{ h_{k,l}^* \mathbf{c}^* \mathbf{r}_{k,l} \},$$

where $\mathbf{c}_k = \text{diag}\{\mathbf{C}_k\}$ is the scrambling sequence corresponding to k^{th} user's j^{th} symbol. The soft IC detector for the conventional CDMA system is reformed as

$$\lambda_{\text{IC}}(u_{n,l}^k; O) \approx \frac{4}{N_0} \text{Re} \{ \mathbf{h}_k^* \mathbf{X}_k^* \mathbf{r}' \},$$

where \mathbf{r}' is the interference cancelled version of the received signal. The matrix \mathbf{X}_k is defined as $\mathbf{X}_k = [\mathbf{x}_{k,1} \ \mathbf{x}_{k,2} \ \cdots \ \mathbf{x}_{k,L}]$, where $\mathbf{x}_{k,l}$ denotes the transmitted chip sequence due to the k^{th} user's j^{th} symbol from the l^{th} path, assuming the BPSK symbol +1 is transmitted. Results are plotted after 4 iterations (excluding the initial coherent MF stage), since convergence has normally been reached by then. For genie-aided algorithms shown in plot (a), we assume, for both systems, i) accurate channel estimation with pilot bits; ii) genie-aided coherent MF in the first iteration such that genie-aided IC can be carried out in the subsequent stages. Simulations are done with

$K = 18$ users and $L_k = 5$ or $L_k = 9$ paths (same for all users). For non-genie-aided algorithms shown in plot (b), simulations are conducted at $E_b/N_0 = 7$ dB for $K = 18$ -user systems with $L_k = 9$ for all users. The imperfect channel estimate can be expressed as $\hat{h}_{k,l} = h_{k,l} + e_{k,l}$, where $h_{k,l}$ is the original channel fading coefficient and $e_{k,l}$ is the channel estimation error modeled as a zero-mean complex Gaussian random variable with variance σ_e^2 . Other parameters for the M -ary system are as in Figure 3. Hence, each information bit is spread to 64 chips. The conventional system has the same code rate and spreading factor: it uses a convolutional code with rate $R_c = 1/8$, generator polynomials $(5, 5, 5, 7, 7, 7, 7)_8$, and free distance $d_f = 21$, see [12], followed by spreading to 8 chips per coded bit and 68×68 block interleaving. The code has roughly the same decoding complexity as the code employed in the M -ary system.

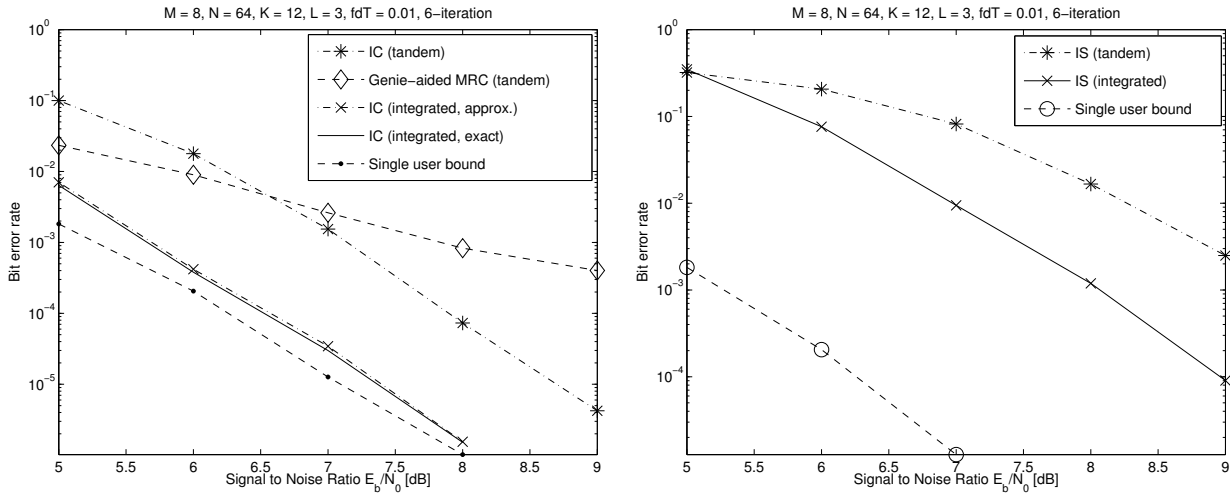
As shown in Figure 4a, for genie-aided algorithms (with perfect CSI), the conventional system outperforms the M -ary system at low SNRs. However, the multipath diversity can be better exploited by the M -ary system, and it outperforms the conventional system at high SNRs. We also observed from our experiments that the performance gain by applying M -ary modulation is more significant in uncoded systems due to the code-spread characteristic of the orthogonal modulation. The plots are omitted here due to space limit. Figure 4b shows the performance comparison of the systems with imperfect CSI. Apparently, channel estimation errors deteriorate the performance for both systems. However, the conventional systems shows slightly more robustness to imperfect CSI as the channel estimation error increases.

V. CONCLUSIONS

We investigate the problem of iteratively demodulating and decoding orthogonally modulated and convolutionally coded signals in frequency selective channels. Among the proposed soft demodulators, the IC demodulator is preferred because it achieves better performance with less complexity compared to the IS soft demodulator. We also show that the M -ary orthogonal CDMA system enables non-coherent detection and decision directed channel estimation, which improves the system spectral efficiency by avoiding the transmission of pilot symbols for channel estimation as in the conventional CDMA systems.

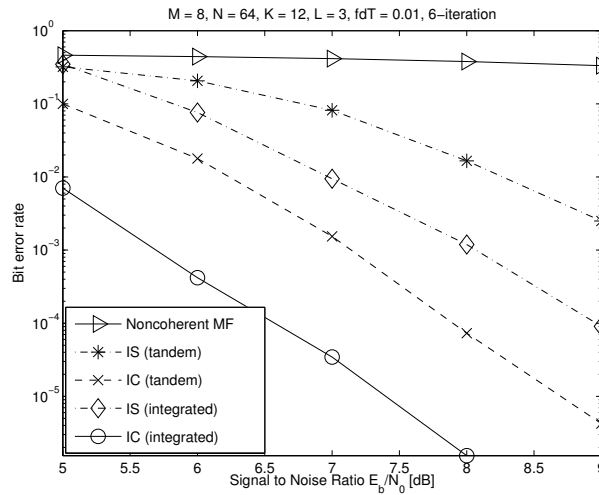
REFERENCES

- [1] K. Pahlavan, M. Chase. "Spread-spectrum multiple-access performance of orthogonal codes for indoor radio communications". *IEEE Trans. on Commun.*, vol. 38, no. 5, pp. 574-577, May 1990.



(a) IC demodulator.

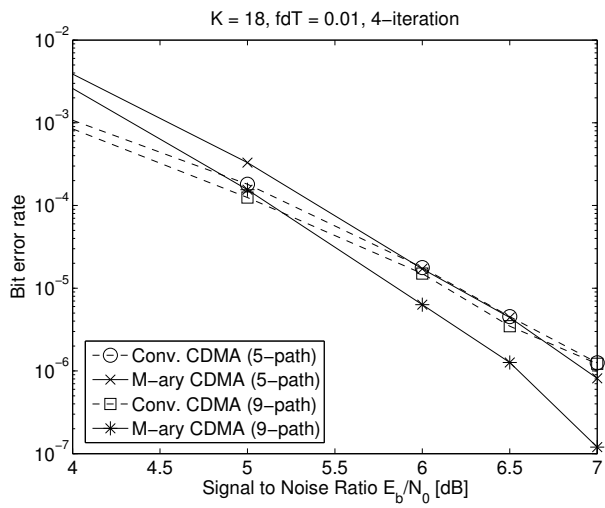
(b) IS demodulator.



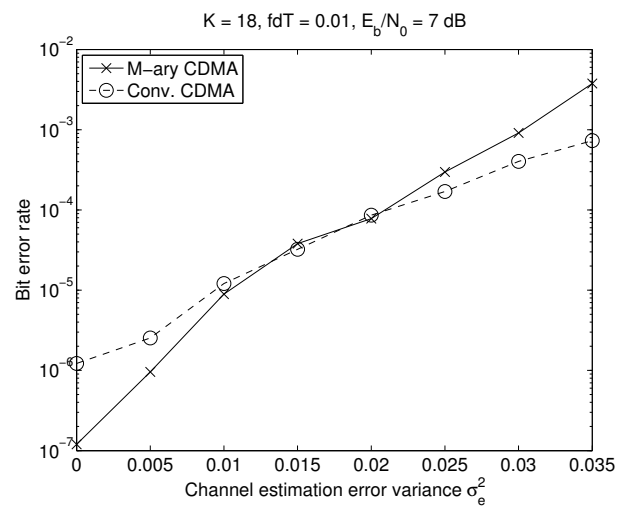
(c) IC vs IS.

Fig. 3. Comparison of different schemes in a $K=12$ -user system.

- [2] P. Enge, D. Sarwate. "Spread-spectrum multiple-access performance of orthogonal codes: linear receivers". *IEEE Trans. on Commun.*, vol. 35, no. 12, pp. 1309–1319, Dec. 1987.
- [3] R. Herzog, J. Hagenauer, A. Schmidbauer. "Soft-in/soft-out Hadamard despreader for iterative decoding in the IS-95(A) system". *Proc. VTC*, vol. 2, pp. 1219–1222, May 1997.
- [4] P. Liang, W. Stark. "Algorithm for joint decoding of turbo codes and M-ary orthogonal modulation". *Proc. ISIT*, pp. 191, June 2000.
- [5] P. Xiao, E. Ström. "A theoretical evaluation of parallel interference cancellation in M-ary orthogonal modulated asynchronous DS-SS system over multipath Rayleigh fading channels". *IEEE Trans. on Veh. Technol.*, vol. 54, no. 4, pp. 1400–1414, July, 2005.
- [6] P. Robertson, E. Villebrun, P. Hoeher. "A comparison of optimal and sub-optimal MAP decoding algorithms operating in the log domain". *Proc. ICC*, pp. 1009–1013, 1995.
- [7] M. Valenti. "Turbo codes and iterative processing". *IEEE New Zealand Wireless Commun. Symp.*, Nov. 1998.
- [8] J. Proakis. *Digital Communications*. McGraw-Hill Book Co, Singapore, 2001, 4th edition.
- [9] G. H. Golub and C. F. van Loan. *Matrix Computations*, 2nd edition, Johns Hopkins University Press, Baltimore, 1989.
- [10] G. W. Stewart. *Matrix Algorithms, Society for Industrial and Applied Mathematics*, 1998.
- [11] P. Xiao, E. Ström. "Correction of extrinsic information for iterative decoding in a serially concatenated multiuser DS-SS system". *IEEE Trans. on Wireless Commun.*, vol. 5, no. 3, pp. 591–602, March 2006.
- [12] P. Lee. "New short constraint length, rate $1/N$ convolutional codes which minimize the required SNR for given desired bit error rates". *IEEE Trans. on Commun.*, vol. 33, no. 2, pp. 171–177, Feb. 1985.



(a) genie-aided algorithms.



(b) non-genie-aided algorithms.

Fig. 4. M-ary CDMA vs. conventional CDMA.